



ELSEVIER

Contents lists available at SciVerse ScienceDirect

Journal of Magnetism and Magnetic Materials

journal homepage: www.elsevier.com/locate/jmmmMagnetic structure and glassiness in $\text{Fe}_{0.5}\text{Ni}_{0.5}\text{PS}_3$ D.J. Goossens^{a,*}, S. Brazier-Hollins^b, D.R. James^b, W.D. Hutchison^c, J.R. Hester^d^a Research School of Chemistry, Australian National University, Canberra 0200, Australia^b School of Engineering, Australian National University, Canberra 0200, Australia^c School of Physical, Environmental and Mathematical Sciences, University of New South Wales at the Australian Defence Force Academy, Canberra 2600, Australia^d The Bragg Institute, Australian Nuclear Science and Technology Organisation, Lucas Heights, NSW 2234, Australia

ARTICLE INFO

Article history:

Received 22 March 2012

Received in revised form

13 November 2012

Available online 23 January 2013

Keywords:

Antiferromagnetism

Layered magnetism

FePS₃

Magnetic glass

ABSTRACT

This work explores the magnetic properties of $\text{Fe}_{0.5}\text{Ni}_{0.5}\text{PS}_3$. The system shows pronounced hysteresis in the magnetic phase transition temperature as a function of the *direction* of the change in temperature. Field cooled/zero field cooled hysteresis is not pronounced. However, the transition temperature between antiferromagnetic and paramagnetic order occurs at approximately 97 K on cooling, but at 138 K on warming, whether the warming is after zero field or field cooling.

This is indicative of magnetic glassiness, and made all the more unusual because all measurements exhibit a transition to a third magnetic phase existing at temperatures below ~ 14 K. The intermediate phase relaxes on a laboratory time scale of the order of 48 min, into an antiferromagnetic state whose magnetic structure is, from neutron diffraction, indistinguishable from the low temperature state. This low temperature state shows magnetic ordering consistent with that observed in CoPS_3 and NiPS_3 . Analysis of the neutron measurements shows that the direction of moments cannot be along the *b*-axis. It is also shown that the moments are unlikely to lie in the *c** direction. Therefore, we suggest that the moments lie along the *a*-axis.

© 2013 Elsevier B.V. All rights reserved.

1. Introduction

The family of two-dimensional magnetic materials $M\text{PS}_3$ where $M=\text{Mn}^{2+}$, Fe^{2+} , Ni^{2+} Zn^{2+} etc shows a wide range of magnetic behaviour [1–7]. Given that $\text{Fe}_{0.5}\text{Mn}_{0.5}\text{PS}_3$ has been found to be a spin glass [2], it was considered to be of interest to explore the behaviour of $\text{Fe}_{0.5}\text{Ni}_{0.5}\text{PS}_3$. The end members, FePS_3 and NiPS_3 , are antiferromagnets with transition temperatures of 123 K and 155 K respectively.

In FePS_3 and NiPS_3 the correlation structure of the spins was thought to be similar [8], with the nature of the anisotropy different. However, more recent work suggests that the magnetic structure of FePS_3 is not yet fully understood [9]. The competing anisotropies – XY in NiPS_3 and Ising in FePS_3 – are also likely to lead to interesting magnetic behaviour. The three-fold in-plane coordination in these honeycomb lattice systems renders geometrical frustration unlikely, despite the significant next-nearest neighbour interactions (for example [10]).

The crystal structure of a typical member of the $M\text{PS}_3$ family, MnPS_3 , is shown in Fig. 1 and shows the honeycomb arrangement of Mn atoms, the P_2 dimers and the layers of sulphur atoms that sandwich the Mn/ P_2 layers. There is a van der Waals gap between these sandwich structures resulting in an indirect exchange path

along *c*, contributing to the 2D magnetic properties and giving the crystals highly anisotropic structural behaviour.

The space group is $C2/m$ and lattice parameters are $a=5.812(2)$ Å, $b=10.070(3)$ Å, $c=6.632(1)$ Å and $\beta=106.98(3)^\circ$ (NiPS_3 , [11]) and $a=5.934(6)$ Å, $b=10.28(1)$ Å, $c=6.772(7)$ Å and $\beta=107.2(1)^\circ$ (FePS_3 , [12]).

A magnetic glass generally occurs when a transition between magnetic states is arrested through some mechanism, such as competing interactions and/or anisotropy. This gives rise to a state consisting of randomly oriented clusters of moments, frozen over time scales of minutes/hours [14]. Three measurements that can be used to distinguish spin glasses and magnetic glasses are:

- Thermal hysteresis: For a magnetic glass a distinct thermal hysteresis occurs between the FCC and FCW susceptibilities (FCC is field cooled cooling — measurement made in a field while cooling the sample and FCW is field cooled warming — measurements made while warming in a field after cooling in a field). For spin glasses, the FCC and FCW curves should be identical.
- Irreversibilities: The thermomagnetic irreversibility of a magnetic glass appears above a critical field (dependent on the material) and increases with increasing applied field. The thermomagnetic irreversibility of a spin glass decreases with increasing applied field.
- Relaxation: The FCC/FCW states of the magnetic glass undergo relaxation towards the equilibrium ZFC state, regardless of applied field.

* Corresponding author. Tel.: +61 2 61253536.

E-mail address: goossens@rsc.anu.edu.au (D.J. Goossens).

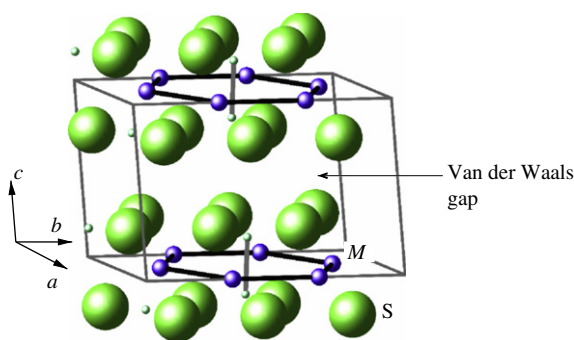


Fig. 1. The crystal structure of MnPS_3 . Large green spheres are S, blue are M and the P_2 pairs are indicated by the dumbbells [13,11]. (For interpretation of the references to color in this figure caption, the reader is referred to the web version of this paper.)

2. Experimental

2.1. Sample preparation

Samples of FePS_3 , NiPS_3 and $\text{Fe}_{0.5}\text{Ni}_{0.5}\text{PS}_3$ were synthesised by direct combination of the appropriate metal sulphides with phosphorus and sulphur. Stoichiometric weights of the powders were thoroughly homogenised using a mortar and pestle, pressed into pellets and sealed inside quartz tubes which were flushed with argon and evacuated to 10^{-3} Torr. To avoid the build up of pressure inside the ampoule, the FePS_3 and NiPS_3 samples were ramped to 700°C over 8 days, before being held at 700°C for 7 and 11 days respectively. The $\text{Fe}_{0.5}\text{Ni}_{0.5}\text{PS}_3$ sample was ramped over 24 days due to larger sample mass, before being held at 700°C for 1 month. It was found that regrinding and a second anneal was required to achieve homogeneity in mixed metal samples such as $\text{Fe}_{0.5}\text{Ni}_{0.5}\text{PS}_3$.

2.2. X-ray diffraction

Powder XRD data were collected on a Siemens D5000 Diffractometer. A monochromator in front of the detector selected out $\text{Cu K}\alpha$ radiation and removed the X-ray fluorescence originating from iron in the sample.

Rietica [15] was used to perform Rietveld [16] and Le Bail [17] fits.

2.3. Electron microscopy

Compositional analysis was undertaken using a Joel 6400 Scanning Electron Microscope (SEM) at the ANU Centre for Advanced Microscopy to determine the composition of $\text{Fe}_{0.5}\text{Ni}_{0.5}\text{PS}_3$. Samples of the end members were also analysed for use as standards.

2.4. Magnetisation measurements

Magnetic susceptibility measurements used a 1.6 T EG&G PARC model number 155 Vibrating Sample Magnetometer (VSM) and closed-cycle helium refrigerator (CCR) at UNSW Canberra Campus. In all experiments the sample was first cooled to 8.0 K in zero applied field. To identify hysteric magnetic behaviour three different measurement protocols were used.

1. Zero Field Cooled Warming (ZFCW): After initial cooling without a field, a field of 1 T was applied and the sample was warmed at a constant rate of 3 K/min to 320 K.
2. Field Cooled Cooling (FCC): The field was maintained and the sample was cooled to 8.0 K. Due to the nature of the CCR, the

cooling rate could not be as tightly controlled as the warming rate, but over the most significant span (200 K to 75 K) was reasonably consistent at -7 K/min.

3. Field Cooled Warming (FCW): The sample was maintained at 8 K for approximately an hour and then field was maintained while the sample was warmed back to room temperature at a constant rate of 3 K/min.

To confirm magnetic relaxation of $\text{Fe}_{0.5}\text{Ni}_{0.5}\text{PS}_3$ the ZFCW and FCC protocols were repeated, however the sample was then cooled to 100 K during the FCC cycle and held at this temperature for 3 h. The sample was a loosely packed powder.

These experiments were repeated (with identical temperature ranges and equivalent cooling/warming rates) with the field applied (1) parallel and (2) orthogonal to the compression direction of a small uniaxially pressed pellet of $\text{Fe}_{0.5}\text{Ni}_{0.5}\text{PS}_3$.

2.5. Neutron diffraction

Neutron powder diffraction data were collected at a wavelength of 1.62158 \AA using the Echidna diffractometer at the OPAL Reactor (Bragg Institute, Australian Nuclear Science and Technology Organisation) [18]. Measurements were made at a range of temperatures in magnetic fields of 0 T and 1 T.

Because of the plate-like shape of the crystallites of $\text{Fe}_{0.5}\text{Ni}_{0.5}\text{PS}_3$, the sample consisted of three uniaxially pressed 6 mm diameter pellets mounted with mutually orthogonal axes. The sample could not be rotated during the experiment. This arrangement ensured that more of reciprocal space was sampled than would have been the case using a single pellet with its strong preferred orientation (so strong that some classes of reflections may be suppressed entirely). However, each of the three pellets had strong preferred orientation, meaning that while the diffraction pattern was more thoroughly sampled, relative peak intensities were not reliable. This means that it was possible to identify and index magnetic reflections of all classes (something that would have been impossible in a highly oriented sample), which allowed determination of the correlation structure of the magnetic moments. However, only limited information could be gained regarding the magnetic moments magnitudes and directions.

The measurements were made while the sample was in its 'relaxed' state to ensure no transient effects were observed. This was achieved by allowing the sample to equilibrate for approximately two hours between successive measurements. This was necessary as the data collection times were long relative to the sample relaxation time, and measurements made while the sample was relaxing would be uninterpretable.

3. Crystal structure

Crystal structures of samples of FePS_3 and NiPS_3 were established to be close to those expected [11,12]. Parameters were established for $\text{Fe}_{0.5}\text{Ni}_{0.5}\text{PS}_3$. Table 1 lists key unit cell parameters. Fig. 2 shows the XRD pattern for $\text{Fe}_{0.5}\text{Ni}_{0.5}\text{PS}_3$, along with a Rietveld fit. Table 2 gives atomic coordinates; atomic displacement parameters (ADPs) and occupancy factors could not be refined reliably due to the strong preferred orientation.

The cell volume of $\text{Fe}_{0.5}\text{Ni}_{0.5}\text{PS}_3$ is close to the average of the volumes of FePS_3 and NiPS_3 . Based on Vegard's law, the experimentally achieved composition $\text{Fe}_x\text{Ni}_{1-x}\text{PS}_3$ is $x = 0.50 \pm 0.03$. SEM-EDX, averaged over a range of crystallites in the powder, gives $x = 0.52 \pm 0.03$, indicating a sample very close to the desired composition.

Table 1
Lattice parameters for FePS₃ (Rietveld refinement), NiPS₃ and Fe_{0.5}Ni_{0.5}PS₃ (Le Bail refinement) in the monoclinic space group C2/m.

Sample	a (Å)	b (Å)	c (Å)	β (°)	V (Å ³)
FePS ₃	5.952(1)	10.305(1)	6.751(1)	107.39(1)	395.1
NiPS ₃	5.817(1)	10.082(1)	6.627(1)	106.91(1)	371.8
Fe _{0.5} Ni _{0.5} PS ₃	5.893(5)	10.193(5)	6.651(5)	106.76(5)	382.5

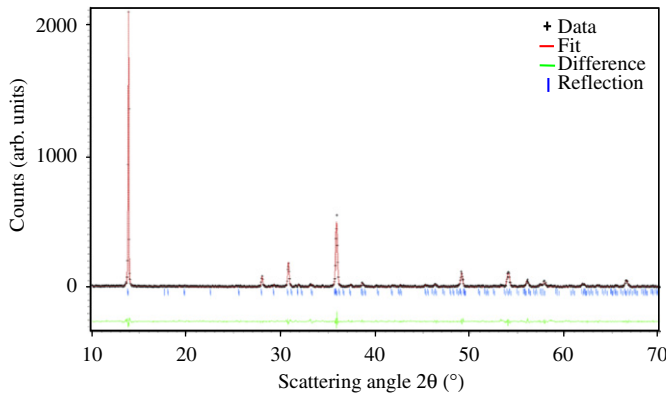


Fig. 2. Le Bail refinement of Fe_{0.5}Ni_{0.5}PS₃ in C2/m from XRD data.

Table 2
Atomic coordinates in Fe_{0.5}Ni_{0.5}PS₃; occupancy and ADPs not refined.

Atom	x	y	z	Occupancy, n (%)
Fe	0	0.327(2)	0	50
Ni	0	0.327(2)	0	50
P	0.040(4)	0	0.121(2)	100
S1	0.730(3)	0	0.239(2)	100
S2	−0.263(2)	0.336(1)	0.244(1)	100

4. Magnetisation measurements

The magnetisation curves of powder samples of FePS₃ and NiPS₃ were measured as functions of temperature after cooling samples in zero field. Samples were heated in applied fields of between 100 mT and 1 T from 4 K to room temperature. The observed transition temperatures agreed with those from the literature. Because of the powder nature of the samples, the parallel and perpendicular susceptibilities could not be separated, and the sample susceptibility, χ , was a combination of the two. The platiness of the crystal habit means it is unlikely that the observations reflect a simple average of $\chi = 1/3\chi_{\parallel} + 2/3\chi_{\perp}$.

Fig. 3 shows the magnetisation measurements for a loosely packed powder of Fe_{0.5}Ni_{0.5}PS₃ at 1 T; measurements made at 100 mT are similar but noisier. Equivalent measurements were made on FePS₃ and NiPS₃ and the hysteresis apparent in Fe_{0.5}Ni_{0.5}PS₃ was not seen. Measurements performed on uniaxially pressed pellets of Fe_{0.5}Ni_{0.5}PS₃ showed hysteresis, suggesting that it is not related to, for example, grain rotation in the applied field. Similarly, the difference between T_C^2 on cooling and warming was not a result of poor heat transfer during the experiment. The results were repeated for independently manufactured and measured samples.

We note that there is some noise in the signal, the result of measuring relatively small antiferromagnetic moments on an instrument more suited to systems with ferromagnetic moments.

The sample shows three magnetic phases—paramagnetism above the cusp at around 97 K (this temperature is denoted T_N^2), and antiferromagnetism below the lower cusp at approximately

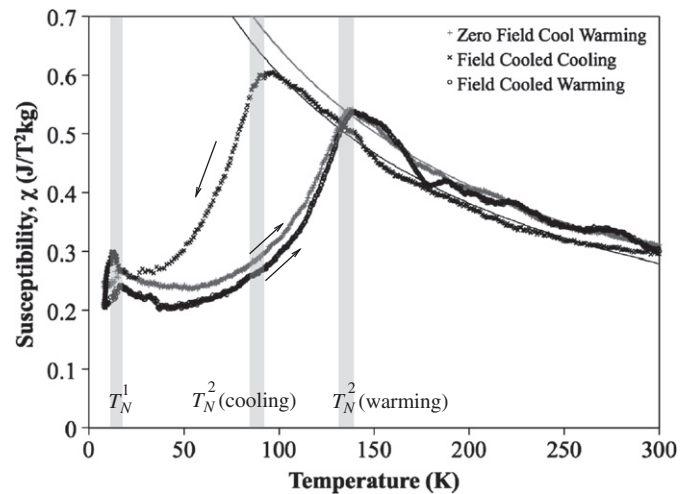


Fig. 3. Magnetic susceptibility of a powder of Fe_{0.5}Ni_{0.5}PS₃, measured in a field of 1 T under a range of conditions. Arrows indicate temperature increasing or decreasing, while the order in which measurements were made: (1) warming after cooling in zero field (ZFCW); (2) cooling in a field (FCC) and lastly; (3) warming after cooling in a field (FCW).

13 K (T_N^1), and an intermediate phase that also appears antiferromagnetic. This is essentially in line with what has been previously observed [19,5], where the two transitions were assigned to different sublattices. However, the earlier work undertook ZFCW and FCW measurements and saw no difference, and concluded that the system was not glassy, as indeed it is not a conventional spin glass. However, Fig. 3 shows that there is pronounced hysteresis as a function of the *direction* of the change in temperature, that is, FCC/FCW (or FCC/ZFCW) hysteresis, as distinct from ZFCW/FCW hysteresis as observed in a conventional spin glass. This is one signature of a ‘magnetic glass’. For conventional spin glasses, the FCC and FCW curves should be identical [14].

While [5] notes that “Magnetic susceptibility measurements were done from 300 K down to 10 K” it can be noted that ZFC measurements *must* be done while warming after cooling in zero field, and thus we do not interpret this comment as meaning that measurements we made on cooling in [5], and thus we believe that there is no discrepancy between that work and results presented here.

Curie–Weiss fits to these (admittedly noisy) data for $T > T_N^2$ give an effective ordered moment of $2.86 \pm 0.06\mu_B$ for all measurements, while for the warming runs $\theta = 77 \pm 1$ K and for the cooling run there is a small difference and $\theta = 73 \pm 1$ K. $2.86\mu_B$ is very close to the quenched moment for Ni²⁺ given by Hund’s rules, whereas an average of Fe²⁺ and Ni²⁺ quenched moments gives $3.87\mu_B$, as observed in [19]. It should be noted however that [19] also suggest different critical temperatures for the Ni and Fe sublattices, or at least different critical temperatures ‘related to’ the sublattices. If this is taken to mean transitions to paramagnetism happen separately on the two sublattices, this would imply different values of θ for Fe versus Ni in a Curie–Weiss fit, as the Fe would be making a paramagnetic contribution from a much lower temperature. It is not clear that this has been catered for in their analysis. If the assumption is made that both Ni and Fe show their quenched moments in the paramagnetic regime, but that Fe ‘disorders’ at a much lower temperature, it is possible to fit the data in Fig. 3 to an expression of the form

$$\chi = \frac{C_{\text{Ni}}}{T + \theta_{\text{Ni}}} + \frac{C_{\text{Fe}}}{T + \theta_{\text{Fe}}} \quad (1)$$

where the usual Curie–Weiss law for an antiferromagnet is $\chi = 2C/(T + \theta)$ and half the magnetic atoms are Fe and half Ni.

Taking the moments of Ni and Fe as $2.83\mu_B$ and $4.90\mu_B$ respectively, and fitting only the θ values in Eq. (1) it is possible to get identically ‘good’ fits to the data as fitting a single Curie–Weiss function in which both C and θ are varied. Hence it is difficult to conclude whether the model in which there are separate sublattices for Ni and Fe is valid.

To gain some insight into the directions of the moments, measurements were made on a uniaxially pressed pellet, with the compression axis parallel and then perpendicular to the applied field. If the moments were close to c^* (as they are in MnPS_3 , where they are at an angle of 8° to c^* [20]) then this should induce a substantial difference between susceptibility measured for the field parallel to the compression direction compared to a perpendicular measurement. However, if the moments are in the plane differences would be less pronounced. As no substantial difference between susceptibility was observed for the two orientations it was determined that the magnetic moments are most likely not aligned along c^* .

Once the first condition for magnetic glassiness was established — the presence of hysteresis — (see Section 1) — a second test was performed to test for relaxation in the system. The sample was cooled in zero field, measured while warming in a field, giving a conventional ZFCW measurement, and the FCC measurement was begun, but the cooling was halted at 100 K—below T_N^2 as observed on warming but above T_N^2 as observed on cooling. The result is shown in Fig. 4.

The relaxation was fitted to a stretched exponential for the form

$$\chi = A + B e^{-((t-t_0)/\tau)^\beta} \quad (2)$$

where A and B scale the fit to the data, t is time, t_0 is the ‘start time’ for the relaxation, τ is the time constant and β is the stretching parameter. The effective mean relation time constant, $\langle \tau \rangle$, is given by

$$\langle \tau \rangle = \frac{\tau}{\beta} \Gamma\left(\frac{1}{\beta}\right) \quad (3)$$

where Γ is the gamma function.

$\tau = 12.5(5)$ s and $\beta = 0.186(6)$ gives $\langle \tau \rangle \sim 48$ min. The fit is extremely good, and suggests that the stretched exponential,

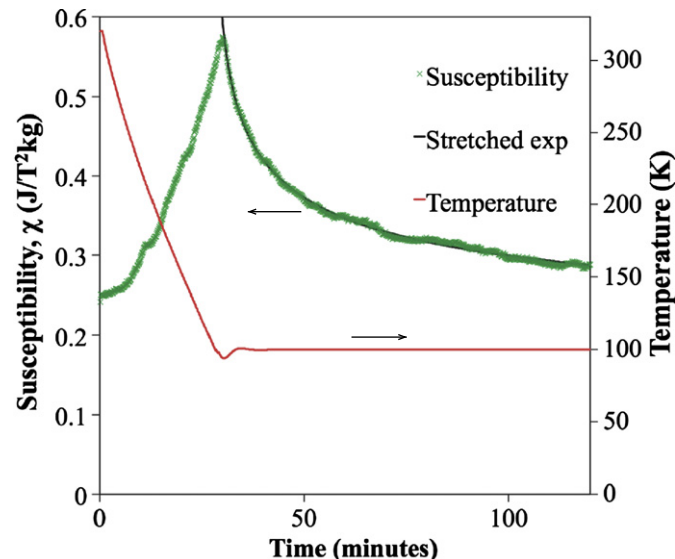


Fig. 4. Relaxation of magnetic susceptibility of a powder of $\text{Fe}_{0.5}\text{Ni}_{0.5}\text{PS}_3$, measured in a field of 1 T at 100 K. Decrease of susceptibility from FCC value to average of ZFCW/FCW values over a period of approximately 2 h.

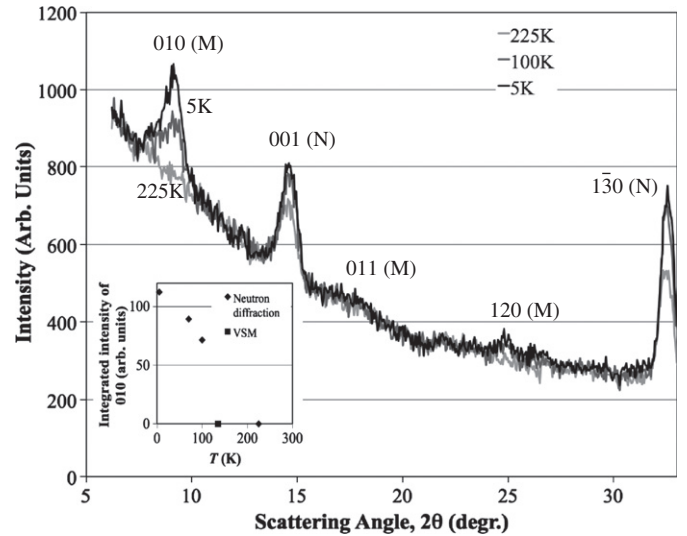


Fig. 5. Low angle region of three diffraction patterns measured with 1.62158 \AA neutrons. Magnetic and nuclear reflections were identified from differences between traces—225 K (lower trace, light grey) 100 K (middle trace, dark grey) and 5 K (upper trace, black) ‘N’ indicates a nuclear reflection, and ‘M’ a magnetic. The 011 is very weak. The inset shows the temperature dependence of the integrated intensity of the 010 peak; the point noted ‘VSM’ gives T_N^2 as given by magnetometry (ZFCW).

which is often used for relaxational phenomena in disordered systems, is appropriate here.

The final value of χ is within error of that seen in the ZFCW experiment, as would be expected for a magnetic glass. This time constant shows the system is far from completely frozen, yet relaxes slowly compared to typical time scales for magnetic susceptibility measurements as a function of T .

5. Neutron diffraction

To identify magnetic diffraction peaks neutron diffraction patterns were collected at 0 K, 70 K, 100 K and 225 K. Purely magnetic diffraction peaks show zero normalised intensity at 225 K as $\text{Fe}_{0.5}\text{Ni}_{0.5}\text{PS}_3$ is paramagnetic at this temperature (see Fig. 5).

The magnetic reflections obey $h+k=2n+1$ which is not allowed for the $C2/m$ space group associated with the crystal structure of $\text{Fe}_{0.5}\text{Ni}_{0.5}\text{PS}_3$. These reflections agree with those for the CoPS_3 and NiPS_3 magnetic structures [21]. The difference between the CoPS_3 and NiPS_3 magnetic structures is the direction of spin, namely along the a -axis and c -axis respectively.

As the 010 magnetic reflection is present in $\text{Fe}_{0.5}\text{Ni}_{0.5}\text{PS}_3$ at low T , the direction of spin of the magnetic moments cannot lie along the b -axis—magnetic reflections with scattering vector parallel to the moment direction show no magnetic structure factor. Results from Section 4 suggest that the moments are unlikely to be aligned along c^* (or c , which is close to but not parallel with c^*). Therefore, the moments are likely to be either aligned along the a axis or an intermediate direction. Preferred orientation prevents the determination of moment magnitude.

These neutron data allow determination of the behaviour of the lattice parameters as a function of T (Table 3). These results show a consistent increase in cell volume, although not all lattice parameters appear to change monotonically. Within error, there is virtually no change in β , and changes in the other parameters are also relatively small compared to the errors.

The magnetic diffraction above and below T_N^1 shows no qualitative difference, but rather a straightforward change in

Table 3

Lattice parameters for $\text{Fe}_{0.5}\text{Ni}_{0.5}\text{PS}_3$ (Le Bail refinement) in the monoclinic space group $C2/m$, with T .

Parameter	RT (XRD)	225 K (neutron)	100 K (neutron)	70 K (neutron)	5 K (neutron)
a (Å)	5.893(5)	5.887(3)	5.863(3)	5.863(2)	5.860(2)
b (Å)	10.193(9)	10.168(5)	10.183(5)	10.182(4)	10.178(3)
c (Å)	6.651(6)	6.668(5)	6.654(6)	6.651(5)	6.647(4)
β (°)	106.79(5)	107.07(5)	107.04(3)	107.02(4)	107.02(3)
V (Å ³)	382.5	381.6	379.8	379.6	379.1

the magnitudes of the Bragg peaks. It appears that the ground state is the same above and below T_N^1 , so the cusp relates to a change in the glassy aspects of the behaviour rather than the equilibrium magnetic ordering.

Neutron diffraction measurements were repeated for all temperatures with the sample in an applied field of 1 T. In all cases, the 1 T and 0 T measurements for a given temperature were indistinguishable. When it is recalled that the sample was allowed to relax before the diffraction measurements were undertaken, this supports the idea that, given time to relax, the field-cooled sample eventually falls into the state obtained on warming the sample, which appears to be the same as the state arising in zero field.

6. Conclusions

Three distinct magnetic phases have been shown for $\text{Fe}_{0.5}\text{Ni}_{0.5}\text{PS}_3$ one at low temperatures below $T_N^1 \sim 14$ K, a second at intermediate temperatures and paramagnetism above $T_N^2 \sim 100$ K. However, T_N^2 is dependent on the *direction* of the ramping of the temperature. Relaxation has also been observed from the FCC state to that of the ZFCW/FCW states over a period of approximately 2 h (time constant of ~ 48 min). Therefore, two of the three requirements for magnetic glass identification have been sufficiently satisfied to conclude that the intermediate phase is likely a magnetic glass, induced by mixed exchange and anisotropy.

Neutron diffraction measurements have shown that the magnetic structure of $\text{Fe}_{0.5}\text{Ni}_{0.5}\text{PS}_3$ is similar to that of CoPS_3 and NiPS_3 . Furthermore, from these measurements it was determined that the direction of the magnetic moments is unlikely to lie along

the b -axis. Magnetic susceptibility measurements have shown that the direction of the magnetic moments are unlikely to lie in the c^* direction either. Therefore, it is suggested that the moments lie along the a -axis.

Acknowledgements

DJG thanks the Australian Institute of Nuclear Science and Engineering (AINSE) for the support of an AINSE Research Fellowship. Many thanks to Assoc. Prof. Glen Stewart of UNSW@ADFA for assistance with magnetisation data. Many thanks also to Dr. Frank Brink of the Centre for Advanced Microscopy at ANU and Prof. A. Lowe of Engineering at ANU for assistance with SEM.

References

- [1] A.R. Wildes, H.M. Rønnow, B. Roessli, M.J. Harris, K.W. Godfrey, *Journal of Magnetism and Magnetic Materials* 310 (2007) 1221–1223.
- [2] Y. Takano, A. Arai, Y. Takahashi, K. Takase, K. Sekizawa, *British Journal of Applied Physics* 93 (2003) 8197–8199.
- [3] S. Ban, Y. Takano, N. Ohkubo, H. Hoya, Y. Takahashi, K. Takase, K. Sekizawa, *Hyperfine Interactions* 165 (2005) 95–99.
- [4] P.A. Joy, S. Vasudevan, *Physical Review B* 46 (1992) 5425–5433.
- [5] R.R. Rao, A. Raychaudhuri, *Journal of Physics and Chemistry of Solids* 53 (1992) 577–583.
- [6] D.J. Goossens, A.R. Wildes, C. Ritter, T.J. Hicks, *Journal of Physics: Condensed Matter* 12 (2000) 1845–1854.
- [7] D.J. Goossens, A.J. Studer, S.J. Kennedy, T.J. Hicks, *Journal of Physics: Condensed Matter* 12 (2000) 4233–4242.
- [8] G.L. Flem, R. Brec, G. Ouvrard, A. Louisy, P. Segransen, *Journal of Physics and Chemistry of Solids* 43 (1982) 455–463.
- [9] K.C. Rule, G.J. McIntyre, S.J. Kennedy, T.J. Hicks, *Physical Review B* 76 (13) (2007) 134402.
- [10] A.R. Wildes, B. Roessli, B. Lebech, K.W. Godfrey, *Journal of Physics: Condensed Matter* 10 (1998) 6417–6428.
- [11] G. Ouvrard, R. Brec, J. Rouxel, *Materials Research Bulletin* 20 (1985) 1181–1189.
- [12] W. Klingenberg, G. Eulenberger, H. Hahn, *Zeitschrift fuer Anorganische und Allgemeine Chemie* 401 (1973) 97–112.
- [13] T.C. Ozawa, S.J. Kang, *Journal of Applied Crystallography* 37 (2004) 679.
- [14] S.B. Roy, M.K. Chattopadhyay, *Physical Review B* 79 (2009) 052407.
- [15] B.A. Hunter, IUCr Commission on Powder Diffraction Newsletter 20 (1998) 21.
- [16] H.M. Rietveld, *Acta Crystallographica* 22 (1967) 151–152.
- [17] A. Le Bail, *Powder Diffraction* 20 (2005) 316–325.
- [18] K.-D. Liss, B.A. Hunter, M.E. Hagen, T.J. Noakes, S.J. Kennedy, *Physica B* 385–386 (2006) 1010–1012.
- [19] V. Manríquez, P. Barahona, O. Peña, *Materials Research Bulletin* 35 (2000) 1889–1895.
- [20] E. Ressouche, M. Loire, V. Simonet, R. Ballou, A. Stunault, A.R. Wildes, *Physical Review B* 82 (2010) 100408.
- [21] A. Brec, *Solid State Ionics* 22 (1986) 3–30.